An NMR, CD, Molecular Dynamics, and Fluorometric Study of the Conformation of the Bradykinin Antagonist B-9340 in Water and in Aqueous Micellar Solutions†

Jan Sejbal,‡ John R. Cann,§ John M. Stewart,§ Lajos Gera,§ and George Kotovych*,‡

Department of Chemistry, University of Alberta, Edmonton AB T6G 2G2, Canada, and Department of Biochemistry, Biophysics and Genetics, University of Colorado School of Medicine, Denver, Colorado 80262

Received June 30, 1995⊗

A detailed NMR, CD, fluorometry, and molecular modeling study of a novel bradykinin antagonist B-9340, containing a novel amino acid D-Igl (α-(2-indanyl)glycine) at position 7, was carried out. The sequence of B-9340 is D-Arg^0-Arg^1-Pro^2-Hyp^3-Gly^4-Thi^5-Ser^6-D-Igl^7-Oic^8-Arg^9, where Hyp is hydroxyproline, Thi is β-(2-thienyl)alanine, and Oic is (3a*S*,7a*S*)-octahydroindole-2-carboxylic acid. The CD results exhibit a striking effect of SDS on the spectrum of the BK antagonist, indicating that interaction with the surfactant induces a folded peptide structure. The interaction of this antagonist with phosphatidylinositol was monitored by fluorometry, indicating that the interaction of the peptide with the lipid is cooperative, and gives a Hill coefficient of 2.3. The two-dimensional proton NMR measurements indicate that B-9340 has no stable secondary structure in water solution and contains about 10−15% *cis* peptide bonds arising from Pro^2, Hyp^3, and Oic^8. In SDS micelles, NMR reveals the existence of two β-turns based on a number of medium-range connectivities that were useful for molecular modeling. The actual molecular modeling and dynamic runs were performed on B-9340 in an environment consisting of a layer of octyl sulfate anions and water. The results indicate that the structure of B-9340 in a micellar environment is characterized by a nonideal βII-turn comprising residues Pro^2 to Thi^5, a nonideal βII′-turn comprising residues Ser^6−Arg^9, and broad folding in the middle part of the molecule. The structure is stabilized by several hydrogen bonds and by a salt bridge between the guanidine moiety of Arg^1 and the carboxyl group of Arg^9, whereas the middle part of the peptide is buried in the micelle. The structure is deposited as Brookhaven PDB file 1 BDK.

Introduction

Bradykinin (Arg^1-Pro^2-Pro^3-Gly^4-Phe^5-Ser^6-Pro^7-Phe^8-Arg^9) (BK) is naturally present in human body fluids and possesses pharmacological activities such as vasodilation and algesic activities.[1−3] It is one of the most potent vasodilators and causes dilation of blood vessels in muscle, kidney, viscera, and various glands and also in the heart and brain.[4] BK may also be associated with the symptoms of the common cold[5,6] and many other inflammatory disorders.

The conformational analysis of BK has been of interest for a long time with the aim of gaining insight into a possible bioactive conformation in solution (see refs 7−10 and references therein). For example, the conformation of BK in 82 mM sodium dodecyl sulfate micelles (SDS) at a pH of 6.8 is characterized by a β-turn involving residues Ser^6-Pro^7-Phe^8-Arg^9.[7] In view of the important physiological and pathophysiological functions of BK, new drugs to combat severe pathologies are being developed by conformational alteration or restriction of the BK molecule. The preparation of these effective antagonists could be important in the treatment of septic shock, asthma, and rhinitis.[3,11] The antagonistic effect has been suggested to be connected with a C-terminal β-turn[8,9,12] or a β-turn comprising residues 2−5.[13] Very recently, as the present study was completed, an NMR conformational study combined with molecular dynamics[14] on the potent BK antagonist HOE 140 (D-Arg^0-Arg^1-Pro^2-Hyp^3-Gly^4-Thi^5-Ser^6-D-Tic^7-Oic^8-Arg^9; Hyp, hydroxyproline; Thi, β-(2-thienyl)alanine; Tic, 1,2,3,4-tetrahydroisoquinoline-3-carboxylic acid; Oic, (3a*S*,7a*S*)-octahydroindole-2-carboxylic acid) showed a βII′-turn comprising residues 6−9 and a βII-turn between residues 2 and 5.

In the present study, we have carried out NMR, CD, and fluorescence studies on the BK antagonist B-9340 (D-Arg^0-Arg^1-Pro^2-Hyp^3-Gly^4-Thi^5-Ser^6-D-Igl^7-Oic^8-Arg^9) (Figure 1) in H_2O and SDS micelles. A model membrane system was chosen for our studies since it has been shown[15] that membrane binding induces a preferred conformation, orientation, and accumulation of peptide on the surface of lipid membranes. The choice of SDS is due to the fact that it is one of the most widely used and studied surfactants (see ref 16 and references therein). CD and fluorometry measurements were also carried out in the phosphatidylinositol model membrane system. All of those experiments may shed light on the conformation of this BK antagonist in membrane-bound environments.

* Address correspondence to: Dr. George Kotovych, Department of Chemistry, University of Alberta, Edmonton, Alberta, Canada T6G 2G2.

† Abbreviations: CD, circular dichroism; COSY, correlation spectroscopy; BK, bradykinin; Boc, *tert*-butyloxycarbonyl; DSS, sodium 2,2-dimethyl-2-silapentane-5-sulfonate; HMQC, heteronuclear multiple quantum correlation spectroscopy; MD, molecular dynamics; NMR, nuclear magnetic resonance; NOESY, nuclear Overhauser enhancement spectroscopy; ROESY, rotating frame Overhauser enhancement spectroscopy; SDS, sodium dodecyl sulfate; TOCSY, total correlation spectroscopy; D-Igl, α-(2-indanyl)glycine; Hyp, hydroxyproline; Thi, β-(2-thienyl)alanine; Oic, (3a*S*,7a*S*)-octahydroindole-2-carboxylic acid.

‡ University of Alberta.

§ University of Colorado School of Medicine.

⊗ Abstract published in *Advance ACS Abstracts,* February 15, 1996.

0022-2623/96/1839-1281$12.00/0

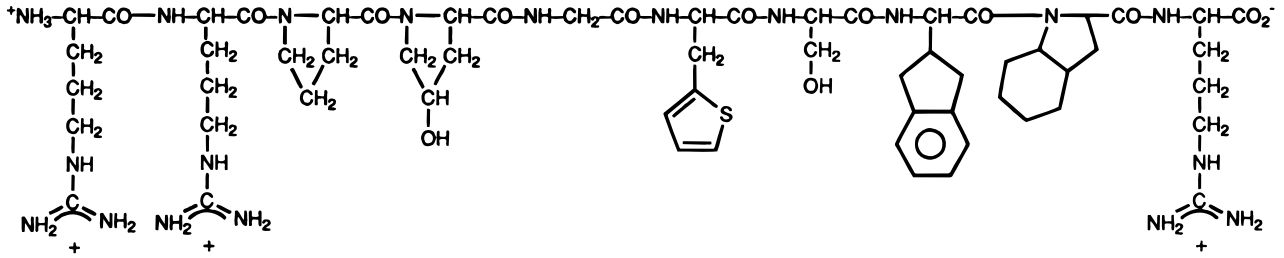

Figure 1. Amino acid sequence of the BK antagonist B-9340: D-Arg^0-Arg^1-Pro^2-Hyp^3-Gly^4-Thi^5-Ser^6-D-IgI^7-Oic^8-Arg^9.

Bradykinin analog B-9340 is important because it was found, unpredictably, to be an effective antagonist at both BK B_1 and B_2 receptors. Two different receptors, B_1 and B_2, mediate the biological actions of BK. B_2 receptors require the entire BK sequence for recognition, whereas B_1 receptors recognize and bind only BK(1−8) or [des-Arg^9]BK. B_2 receptors are expressed constitutively and mediate most normal actions of BK. In chronic inflammation and in sepsis, B_1 receptors are expressed, and contribute an important part to the complex pathophysiological reactions that ensue. Although the amino acid sequences of both B_1 and B_2 receptors are known, knowledge of the conformations of the receptor proteins and the modes of interactions of agonists and antagonists with these receptors is based largely on conjecture and modeling.

Heretofore BK antagonists have been selective for B_1 or B_2 receptors, depending on the absence or presence of the arginine residue in position 9. B-9340, which possesses the Arg^9 residue, was not expected to interact with B_1 receptors, but it was found to be a potent B_1 antagonist. This is particularly surprising, since the only difference between B-9340 and HOE-140, the most potent B_2 antagonist published, is the nature of the amino acid residue at position 7: D-α-(2-indanyl)glycine replaces D-tetrahydroisoquinoline-3-carboxylic acid.

The extensive experimental and modeling studies already done on BK antagonists having structures very similar to that of B-9340 provide the setting for similar studies on this new analog having both B_2 and B_1 antagonist activity. Peptide conformation must surely be an important factor in the B_1 antagonist activity of this new BK analog.

Materials and Methods

Materials. The synthesis of BK antagonist B-9340 was carried out by standard solid phase procedures,[17,18] using Boc amino acids. Coupling reactions were mediated by the BOP reagent (benzotriazol-1-yl)(tris(dimethylamino)phosphonium hexafluorophosphate) in dimethyl formamide.[19] After hydrogen fluoride cleavage, the peptide was purified by countercurrent distribution for 100 transfers in the system 1-butanol: ethyl acetate:1% trifluoroacetic acid (1:1:2). The product was characterized by analytical HPLC, amino acid analysis, TLC, and laser desorption mass spectroscopy.

α-(2-Indanyl)glycine was synthesized by the literature procedure[20] and was resolved enzymatically by hydrolysis of the *N*-acetyl derivate with hog kidney acylase-1. It was converted to the Boc derivative by the standard method. Sodium dodecyl sulfate (SDS) was the electrophoresis purity reagent (>98% C12) of Biol. Rad Laboratories, Richmond, CA, and the nonionic surfactant octaethylene glycol mono-*n*-dodecyl ether (C12E8) manufactured by Nikko Chemical Co., Ltd., Tokyo, Japan, was purchased through the Kouyoh Trading Co., Ltd., Tokyo, Japan. Phosphatidyl inositol was obtained from Sigma Chemical Co., St. Louis, MO. The D_2O was obtained from General Intermediates of Canada, Edmonton, AB; sodium 2,2-dimethyl-2-silapentane-5-sulfonate (DSS) from Merck, Darmstadt, Germany; and deuterated SDS from Cambridge Isotope Laboratories, Woburn, MA.

NMR. The BK antagonist B-9340 (MW 1318, 2.7 mg) was dissolved in the mixture of 500 μL of H_2O and 50 μL of D_2O resulting in sample A. Deuterated SDS (49 mg), 500 μL of H_2O, 50 μL of D_2O, and 5.1 mg of the peptide were used to prepare sample B. The pH of the solutions was measured with a Cole-Parmer C5990 electrode, designed for 5 mm NMR tubes, and was adjusted to 6.0 for the water sample and 6.8 for the sample with SDS by adding small volumes of 0.1 M phosphate buffer components**.** The solutions were filtered, transferred to 5 mm NMR tubes, and then deoxygenated by a stream of argon gas. About 10 μL of a 0.1% solution of DSS in water was added to both samples as internal standard. Sample A was about 3.7 mM in peptide, and the concentration of sample B was about 7.0 mM in peptide and 280 mM in deuterated SDS, high above the critical micellar concentration of this detergent (8 mM). Because the DSS is probably partly incorporated into the micelles, thus providing two resonances instead of one, a concentration dependency of the intensity of these two signals was carried out with the result that the sharper upfield signal belongs to the nonincorporated standard reference peak.

All NMR experiments were carried out on a Varian UNITY 500 spectrometer using a proton-selective 5 mm probe with a 90° proton pulse length of 9.5 μs at a transmitter power of 60 dB. The 90° pulse was checked at the beginning of every session at the spectrometer, and the temperature was always controlled throughout the experiments to ±0.1 °C. For data collection and processing, VNMR 3.1 and 3.2 software was used on the Sun Sparc 4/330 and the Sun Sparc 4/470 workstations, respectively. All 2D spectra were acquired nonspinning, whereas for one-dimensional experiments the spinner was turned on. The temperature coefficients of the amide protons were calculated by analyzing the chemical shifts of sample B at 5.0, 15.0, 25.0, 35.0, and 45.0 °C by means of linear regression. Proton 1D-NMR spectra of two diluted samples (0.7 mM of peptide and 28 mM or 280 mM of SDS) were recorded to confirm that the BK antagonist B-9340 does not aggregate under the conditions used for the 2D experiments. Two-dimensional NMR experiments were carried out at 15, 25, and 35 °C for sample B and at 25 °C for the aqueous sample A. Except for the COSY experiment, they were carried out in the phase-sensitive mode by using the hypercomplex technique known as the States−Haberkorn−Ruben method.[21] In all cases the decoupler and transmitter offsets were set equal, a sweep width of 5000 Hz was used in both dimensions, and typically 4K data points in t2 and 512 experiments in t1 (zero-filled to 2K) were acquired. All two-dimensional experiments were preceded by eight dummy scans, but none were applied between individual t1 increments. The preacquisition delay alfa was individually adjusted, and first point distortions caused by analog filters were compensated by reducing the first point of each FID and of each t1 interferogram by empirically determined values for every 2D experiment. This procedure made the use of any further baseline corrections unnecessary. Water suppression was achieved by weak 1.5 s presaturation before the first pulse of the sequence and for the whole sequence except during acquisition.

The TOCSY experiments[22,23] were carried out by using the basic pulse sequence proposed by Bax. Solvent suppression was achieved by presaturation of the water signal during a 1.5 s relaxation delay. A 2 ms trim pulse preceded the 30 ms

Table 1. 500 MHz ^{1}H NMR Chemical Shifts[a] and Coupling Constants (Hz) of BK Antagonist B-9340 in Water

	NH	H_α	H_β	H_γ	other H	J_{NH} Hα
D-Arg^0		3.93	1.86, 1.86	1.63, 1.63	δ,δ': 3.21, 3.21; NH: 7.97	
		(3.87)	(1.51, 1.45)	(1.36, 1.21)	(2.78, 2.78, 7.89)	
Arg^1		4.56	1.71, 1.71	1.61, 1.61	δ,δ': 3.07, 2.95	
		(4.60)	(1.78, 1.72)	(1.65, 1.65)	(3.12, 3.12)	
Pro^2		~4.8	2.33, 2.01	2.01, 1.85	δ,δ': 3.84, 3.47	
		(~4.8)	(2.35, 2.03)	(2.03, 1.89)	(3.86, 3.53)	
Hyp^3		4.62	2.32, 2.04	4.62	δ,δ': 3.82, 3.82	
Gly^4	8.68	4.01, 3.89, $J_{gem} = 16.5$				
	(8.61)	(3.95, 3.95)				
Thi^5	8.05	4.56	3.29, $J_{\alpha\beta} = 7.4-3.35$, $J_{\alpha\beta} = 6.7$, $J_{\beta\beta'} = 15.0$		Ar: 3′: 6.92; 4′: 6.98; 5′: 7.30, $J_{3',4'} = 3.4$, $J_{3',5'} = 1.1$, $J_{4',5'} = 5.1$	
	(8.07)	(4.61)	(3.31, 3.38)		(3′: 6.96; 4′: 7.01; 5′: 7.32)	
Ser^6	8.24	4.45	3.66, 3.73, $J_{\alpha\beta} = 8.4$, $J_{\alpha\beta'} = 5.7$, $J_{\beta\beta'} = 11.6$			8.4
	(8.29)	(4.39)	(3.81, 3.82)			
D-Igl^7	7.93	~4.8	2.82	2.64 ($J_{\alpha\beta} = 5.8$) and 3.02 ($J_{\alpha\beta} = 7.3$), $J_{gem} = 16.0$, 2.77 ($J_{\alpha\beta} = 5.7$) and 3.01 ($J_{\alpha\beta} = 7.2$), $J_{gem} = 13.5$	Ar: 3′,6′: 7.31; 4′,5′: 7.23	
	(8.17)	(4.33)	(2.95)	(2.57 and 3.06, 2.59 and 2.95)	(3′6′: 7.32; 4′5′: 7.22)	
Oic^8		4.46	2.28, 2.02	2.49	δ: 3.87 4_{pro-R}: 1.77; 4_{pro-S}: 1.63; 5_{pro-R}: 1.24; 5_{pro-S}: 1.45; 6_{pro-R}: 1.08; 6_{pro-S}: 1.63; 7_{pro-R}: 1.93; 7_{pro-S}: 1.49	
Arg^9	7.97	4.15	1.86, 1.84	1.66	δ,δ': 3.21; ϵNH 7.18	
	(7.93)	(4.16)	(1.86, 1.84)	(1.66)	(δ,δ': 3.20)	

[a] At 25 °C, in δ scale relative to internal DSS = 0. Chemical shifts in brackets belong to the less populated isomer.

MLEV-17 spin-lock at a field strength of 5.0 kHz. A total of 64 scans were accumulated per t1 increment, and connectivities from the amide proton to $H_{\delta,\delta'}$ of all arginine residues were readily observed. Usually, π/4-shifted sine bell apodization functions were used in both dimensions. The ROESY experiment (sample A) was recorded with the pulse sequence 90°−t1−90°−SL−90°−FID.[24,25] Spin-lock (SL) conditions were achieved by a series of hard pulses of 32° flip angle and the 90° pulses immediately preceding and following the spin-locking period were added to compensate for the non-negligible offset dependence of the cross peaks (compensated ROESY). The experiments were carried out with a mixing time of 100 ms and 48 scans per FID were acquired. Care was taken to avoid homonuclear Hartmann−Hahn (HOHAHA) effects. Because the effectiveness of HOHAHA magnetization transfer depends directly on the effective rf field strength, the strength of the applied spin-lock was chosen quite low at 2.5 kHz providing suitable peak intensities with basically no HOHAHA contributions. COSY spectra[26] were measured in the absolute value mode, and for resolution enhancement the combination of nonshifted sine bell and negative exponential were used as the weighting function. The NOESY experiments[27] were carried out in the standard manner using 2.5 s delay with 1.5 s presaturation of the water signal and mixing times of 150, 250, and 400 ms with 64 transients per increment and 400 increments. A standard 90°−t1−90°−mix−90°−FID pulse sequence and a shifted sine bell weighting function were used in both dimensions.

Signal assignment in individual residues and backbone was based on TOCSY, COSY, and NOESY or ROESY spectra.[28] For assignment of signals in Oic the HMQC experiment[29] with broad band decoupling of ^{13}C during acquisition was also used. Assignment of protons on the thiophene ring in Thi is based on values of coupling constants and on comparison with data taken from the literature.[14] For D-Igl, α-(2-indanyl)glycine, only pairs of geminal γ-protons can be assigned because of lack of spatial information from NOESY or ROESY and overlapping signals. Assignment of Oic is based on published data,[12,14] as well as HMQC, COSY, and NOESY or ROESY spectra and some coupling constants available from one-dimensional spectra. Results are given in Tables 1 and 2 for 25 °C. The nomenclature of Oic and D-Igl is given in Figure 2.

Distances were calculated from NOESY spectra with a mixing time of 150 ms for all nontrivial cross peaks by integration of their 3D volumes. For diminishing the effect of nonequivalent correlation times of various parts of the molecule we use the following: The arithmetic mean of the diastereotopic β protons of Pro^2 and Oic^8 was used as the reference (1.78 Å) for backbone restraints; one nonoverlapping pair of geminal γ-protons of D-Igl^7 was used as the same reference for restraints comprising only protons in freely rotating side chains. Distance constraints to one of two nonassigned geminal protons were applied to the adjacent carbon atom.[30]

All calculations were performed using the program BIOGRAF (Version 3.2.1, Molecular Simulations, Inc., Burlington, MA) on the Sun Sparc 470 Workstation (Sun 4.1.3 operating system, 32 MB operating memory) using the DREIDING II force field method. Data were transferred to the program Hyperchem (Release 2, Autodesk, Inc.) after the calculations were finished for printing the structure. For all energy minimizations the conjugate-gradient method was used; usually 300−400 steps were needed for convergence (less than 0.1 kcal mol^{-1} rms force). Distribution of charges was computed by the Gasteiger method.[31] The default harmonic term for constraints was used. Cutoff distance for nonbond list calculation was 9 Å. The molecular dynamic runs were performed with a 1 fs step. The current structure was written to a trajectory file every 0.1 ps without minimization. Every 0.1 ps lists of nonbond interactions and hydrogen bonds were updated. All simulations were carried out for the molecule with all hydrogens. The dielectric constant of vacuum ($\epsilon = 1$) was used for all calculations for the unsolvated molecule as well as the value for water ($\epsilon = 80$).

For the preliminary estimate of the conformer energies, a Monte Carlo search on torsion angles was used: 800 conformers were generated and minimized in vacuum ($\epsilon = 1$) with all atoms movable. Each conformer was minimized (500 steps *in vacuo*) using all NOE restraints and a maximum force 1000 kcal/Å·mol for this energy term. The 30 lowest energy conformers were minimized again without constraints to relax the molecule (300 steps with $\epsilon = 80$ and then 300 steps with $\epsilon = 1$). Two molecular dynamic (MD) runs were performed starting from the best energy conformer from the Monte Carlo

Table 2. 500 MHz ^{1}H NMR Chemical Shifts,[a] Coupling Constants (Hz), and NH Temperature Coefficients[b] of BK Antagonist B-9340 in 280 mM SDS Solution

	NH	H_α	H_β	H_γ	other H	J_{NH} H_α	tc[b]
D-Arg^0		4.06	1.83, 1.94	1.75, 1.75	δ,δ': 3.22; ϵNH: 7.22		
Arg^1	8.64	4.38	1.78, 1.85	1.69, 1.69	δ,δ': 3.28; ϵNH: 7.23		−4.1
Pro^2		4.77	2.44, 2.07	2.00, 1.92	δ,δ': 3.43, 3.91		
Hyp^3		4.51	2.11, 2.33	4.64	δ,δ': 3.90, 4.02		
Gly^4	8.51	4.02, 3.91				∼5.5	−6.1
Thi^5	7.87	4.75	3.46, 3.21		Ar: 3′: 7.01; 4′: 6.91; 5′: 7.05, $J_{3',4'} = 3.5$, $J_{3',5'} = 0.9$, $J_{4',5'} = 5.1$	7.0	−2.7
Ser^6	8.30	4.42	3.90, 3.72			7.8	−4.0
D-Igl^7	7.57	4.23	2.80	2.55 and 3.05 ($J = 13.4$), 2.65 and 3.04 ($J = 13.5$)	Ar[c]: 4: 7.25 d ($J = 6.5$); 5: 7.11 m; 6: 7.12 m; 7: 7.21 d ($J = 5.9$)	4.5	−4.3
Oic^8		4.59	2.01, 2.42	2.42	δ: 3.55 $4_{pro\text{-}R}$: 1.88; $4_{pro\text{-}S}$: 1.49; $5_{pro\text{-}R}$: 1.34; $5_{pro\text{-}S}$: 1.40; $6_{pro\text{-}R}$: 0.79; $6_{pro\text{-}S}$: 1.63; $7_{pro\text{-}R}$: 2.01; $7_{pro\text{-}S}$: 1.34		
Arg^9	7.59	4.11	1.80, 1.94	1.69, 1.69	δ,δ': 3.20; ϵNH: 7.14	7.5	−2.3

[a] At 25 °C, in δ scale relative to internal DSS = 0. [b] The temperature coefficients of the amide protons are listed in ppb/°C. They are the result of a linear regression analysis of the chemical shifts measured at 5, 15, 25, 35, and 45 °C and accurate to within ±0.2 ppb/°C. [c] Aromatic protons are not assigned stereospecifically.

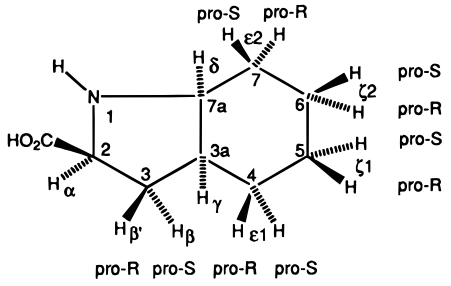

Oic – octahydroindole-2-carboxylic acid

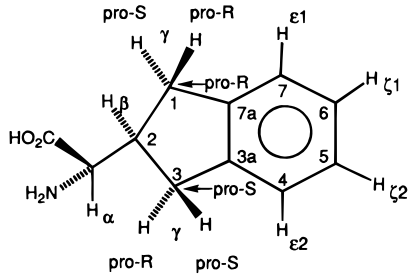

Igl – α-(2-indanyl)glycine

Figure 2. Nomenclature used for Oic and Igl amino acid residues.

search. First of all, for the water environment the following protocol was used: The peptide conformer was solvated with water (diamond grid, 2.8 Å distance between the solvent molecules, trimolecular shell, 287 molecules of solvent), and the resulting system was minimized. The minimized structure was subjected to a 15 ps molecular dynamic run at 300 K. Coordinates from the last 10 ps of trajectory were collected, averaged, and minimized to 0.01 kcal mol^{-1} residual RMS force. All calculations were performed without the application of any constraints.

The second simulation partly emulated a micellar environment. A matrix of 7 × 7 parallel-oriented anions of monooctyl sulfate with a zigzag conformation of the hydrocarbon chain was generated with distances between neighboring chains of 2.5 Å. Minimization of this matrix (2000 steps) led to a fan-shaped formation caused by the repulsion of negatively charged groups on one end of the chains. The conformer from the Monte Carlo search was placed near the central alkyl sulfate anion, and the peptide was solvated with a trimolecular shell of water molecules (diamond grid, 2.8 Å distance between solvent molecules, 2.6 Å inner cutoff of shell from peptide and detergent, 8.5 Å outer cutoff; positions for 212 molecules of solvent were generated). The resulting system was minimized

Table 3. Restraints Used for Molecular Modeling[a]

protons	distance	protons	distance
Gly^{4}NH−Thi^{5}NH	3.1	Ser^{6}NH−D-Igl^7γH[b]	4.0
Thi^{5}NH−Ser^{6}NH	2.6	Pro^2δH−Hyp^3αH	2.9
Ser^{6}NH−D-Igl^{7}NH	2.1	Pro^2δH−Hyp^3γH	2.9
Ser^{6}NH−D-Igl^7αH	3.8	Thi^{5}5H−Oic^8βH	3.6
Hyp^3αH−Thi^{5}NH	3.6	Thi^{5}3H−D-Igl^7γH[b]	3.9
D-Igl^7αH−Arg^{9}NH	3.7	Thi^{5}4H−D-Igl^7γH[b]	3.7
Ser^{6}NH−D-Igl^7βH	3.5	Thi^{5}5H−D-Igl^7γH[b]	3.2

[a] Distances (in Å) calculated from the NOESY spectrum of BK antagonist B-9340 in 280 mM solution of SDS. [b] Approximately the same NOESY volumes for all four γ protons. Therefore, the average value is given.

by applying all distance constraints given in Table 3 to a residual rms force of 0.15 kcal mol^{-1}. Four successive dynamic runs were then performed. The system was heated from 200 to 400 K in 10 ps, then cooled to 300 K during 5 ps, and equilibrated during 30 ps at 300 K. Finally, an 80 ps dynamic run was performed, and the data were collected on disk. The coordinates of 800 structures in the trajectory were averaged, and the resulting structure was minimized at first with constraints (1000 steps) and then without constraints (2000 steps) to relax the molecule from distortions caused by errors in the determination of interatomic distances from the NOESY data. An additional unconstrained dynamic run of overall length 120 ps was performed at 300 K starting from the averaged and minimized structure from the previous constrained dynamic run. The average structure was extracted from the final 60 ps (600 conformers) and then minimized.

The Monte Carlo search and all dynamic runs were performed in the background on the Sun 4/470 data station and took approximately 70% of CPU time averaged over 24 h. One minimization step of the system with peptide, micelle, and water took 11.8 s, one step of the dynamic run 5.7 s. All calculations and interactive manipulations with data represent about 3 weeks of computer time.

CD and Fluorometry. Solutions of B-9340 in SDS or in phosphatidylinositol solubilized with C12E8 were prepared as described previously for BK.[32,33]

CD spectra were recorded at 27 ± 0.05 °C in a thermostated cell holder on a Cary model 60 spectropolarimeter with a model 6001 circular dichroism attachment. The instrument had been modified to eliminate possible artifactual signals on passing through intense absorption bands. The slits were programmed for 1.5 nm band width at each wavelength. The instrument was calibrated with dextro-10-camphorsulfonic acid according to the described procedure.[34] The path length was 0.5−2 cm depending upon solute concentrations and wavelength range. Mean residue ellipticities, $[\theta]$ (deg cm^2 dmol^{-1}), were calculated in the usual fashion using the mean residue weight of 131.8 calculated from the molecular weight of BK antagonist B-9340. Each spectrum is the average of two scans.

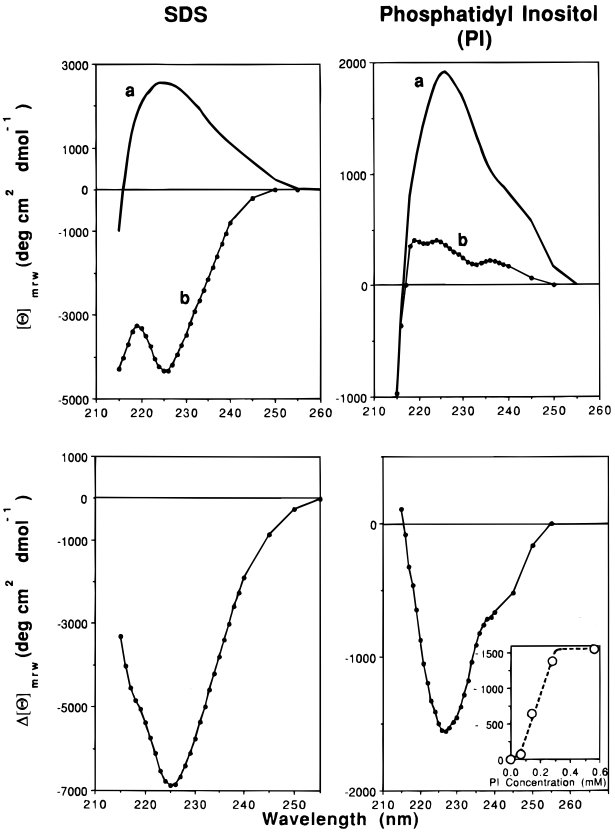

Figure 3. Circular dichroism spectra and corresponding difference spectrum of BK antagonist B-9340 in SDS and in phosphatidyl inositol (PI) solutions as designated by banners. SDS (Upper panel): a, spectrum in water; b, in 82 mM SDS. (Lower panel): Difference spectrum in SDS referred to water. Concentration of antagonist B-9340, 78 μM; pH 6.8. Phosphatidylinositol (Upper panel): a, control spectrum in 1.86 mM C12E8; b, 0.56 mM PI solubilized in 1.86 mM C12E8. (Lower panel): Difference spectrum in solubilized PI referred to control; inset, titration of B-9340 with PI. Concentration of B-9340, 24.8 μM; pH 7.0.

Fluorescence measurements were made on a Farrand Mark I spectrofluorometer. The temperature of the cell was maintained at 27 ± 0.02 °C, utilizing a circulating water bath. Excitation and emission slits were 4 and 8 nm, respectively. The enhancement of the fluorescence intensity of the BK antagonist B-9340 by phosphatidylinositol was corrected empirically for internal absorption (i.e., light scattering of the micellar reaction mixture) by subtraction of the slight fluorescence intensity shown by the same concentration of lipid in the absence of the antagonist.

Results and Discussion

CD and Fluorometry. The CD results displayed in Figure 3 exhibit a striking effect of SDS on the spectrum of the BK antagonist B-9340, indicating that interaction with the surfactant induces a folded peptide structure. In fact, the difference spectrum of the peptide in SDS referred to water is suggestive of a β-turn conformation.[35−37] This is a provocative result since it has been postulated[38] that small peptide−SDS complexes may be a reasonable model for peptide−membrane lipid interactions. With this in mind, measurements were made on the interaction of the antagonist with the membrane lipid phosphatidylinositol.

As shown by the CD measurements presented in Figure 3, the lipid also induces a change in the conformation of the peptide, albeit less so than does SDS, and the difference spectrum is also suggestive of a

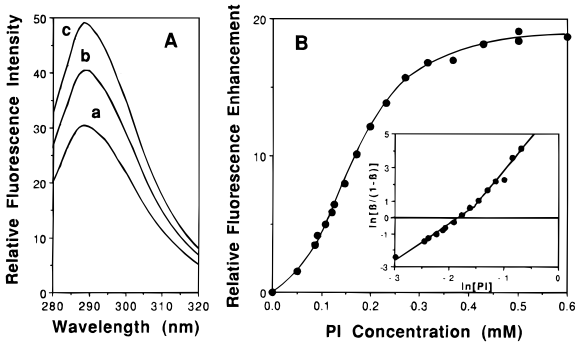

Figure 4. Interaction of BK antagonist B-9340 with phosphatidylinositol (PI) at pH 6.9 as monitored by fluorometry. (A) Effect of PI on the emission spectrum of 24.8 μM antagonist in 1.86 mM C12E8, excitation wavelength 264 nm: a, curve a, 0.0 PI; curve b, 0.170 mM; c, 0.600 mM. (B) Titration of 24.8 μM antagonist with PI: Plot of fluorescence enhancement at 289 nm vs constituent concentration of PI; inset is a Hill plot of the titration data, the fraction saturation β reckoned using the enhancement at 0.6 mM PI (equal, within experimental error, to the average of the two measurements at 0.5 mM) as the end point.

β-turn. Titration of the antagonist with the lipid (inset to the lower panel of the right hand column) gave a midpoint concentration of 0.18 mM phosphatidylinositol, which is to be compared with the midpoint concentration of 0.37 mM in the case of bradykinin, with all else held constant (see ref 32, and a duplicate titration made in the current study). Thus, the bradykinin antagonist interacts twice as strongly with the lipid as does bradykinin. This interesting finding appears to be consistent with a proposed mechanistic principle of peptide−receptor recognition; namely, the lipids of the target cell membrane exert conformational and other constraints on the peptide, enabling it to find its surface receptor and to expedite specific binding.[39]

The interaction of the BK antagonist B-9340 with phosphatidylisositol was monitored additionally by fluorometry, the fluorescence of the peptide owing its origin to the D-Igl residue (data on the free amino acid not shown). The relative fluorescence intensity of the peptide is enhanced upon interaction with graded concentrations of the lipid. As illustrated in Figure 4A, the salient feature of the resulting emission spectra is the insignificant changes in band shape and wavelength of maximum emission. The titration curve is presented in Figure 4B as a plot of relative fluorescence enhancement at λ_{max} = 289 nm against lipid concentration. It is immediately apparent that the interaction of the peptide with the lipid is cooperative. The Hill plot of the data (inset to Figure 4B) could be fitted by two intersecting straight lines, the left hand segment passing through the midpoint of the titration at 0.16 mM lipid in good agreement with the midpoint concentration shown by the CD titration. The slope of the line at the midpoint gives an apparent Hill coefficient of 2.3. These results are indicative of a cooperative, two-state system consisting of free, unstructured peptide and structured peptide bound to lipid−C12E8 mixed micelles. BK itself interacts with monomeric SDS cooperatively.[33] Another example of cooperative binding is provided by membrane proteins and lipids.[40] The cooperative interaction is consistent with the CD finding that binding induces a change in peptide conformation, while the large Hill coefficient might reflect electrostatic binding of the three

guanidine groups of the peptide with phosphate groups on the surface of the micelles. Finally, the unusual shape of the Hill plot may reflect the change in size and in size distribution of the mixed micelles of phosphatidylinositol and C12E8 on going from low to relatively high concentration of lipid as observed by electron microscopy.[32] At 0.186 mM lipid, the micrograph showed a fairly uniform population of 160 Å diameter micelles with a "basket weave" structure. In contrast, at 0.560 mM lipid the micrograph showed a heterogeneous population of 160−700 Å diameter micelles of the same structure.

The importance of using SDS micellar solutions for the NMR study arises from the fact that SDS micelles provide a good interface for the folding of surface-active peptides (see refs 15, 16, and 41 and references therein). An important requirement is that there must be sufficient SDS to bind all of the BK antagonist.[42] Therefore, we estimated the ratio of free peptide to peptide-bound SDS under our experimental conditions. Using a value of $2K_1 = 1.0 \times 10^3$ M^{-1} for the equilibrium association constant ($K_1 = 5 \times 10^2$ M^{-1} is known for the binding of BK by SDS[32] and the factor of 2 comes from the fact that BK-9340 binds twice as strongly to phosphatidylinositol as does BK itself, as discussed above), a total peptide concentration of 7 mM and a total SDS concentration of 280 mM, the results indicate that 99.6% antagonist is bound. This is a lower limit and meets the above-mentioned criterion. Secondly, an estimate was made of the shape, size, and total concentration of SDS micelles. Using the published X-ray scattering results at 25 °C,[43] the micelles in the 280 mM SDS solution are spheres with a radius of 24.0 Å, composed of $n = 67$ monomeric SDS molecules. The total micellar concentration is 4.18 mM and, on the average, 1.7 BK antagonist B-9340 molecules are bound on each SDS micelle. Finally, it is known that NMR spectra in SDS solutions exhibit some line broadening[41] since the interaction of the BK antagonist with the micelles, which have a longer correlation time, leads to short T_2 (transverse relaxation time) values, resulting in broader resonances. This was observed in the case of the BK antagonist HOE 140[14] (to be discussed later), and our experimental conditions were chosen to be very similar to this study. For example, based on one dimensional spectra in the present study, typical line widths at half height for the NH protons at 25 °C are as follows: Gly[4], 11 Hz; Thi[5], 7 Hz; Ser[6], 8 Hz; D-Igl[7], 8 Hz.

We now examined the peptide−SDS interaction using NMR to confirm a β-turn peptide structure in micellar SDS solution.

NMR. The NOESY spectrum of the BK antagonist B-9340 in water at 27 °C shows only a few very weak interactions. Medium cross peaks are present only in the case of some pairs of geminal protons, namely the γ protons of D-Igl[7] and δ protons of Pro[2], showing that these side chains have a different correlation time than the rest of the molecule. In the ROESY spectrum, only sequential cross peaks are present, not only for the main conformer but also for minor components caused by *cis*−*trans* isomerization of proline-like residues Pro[2], Hyp[3], and Oic[8]. The percentage of *cis* peptide bonds can be calculated from the nonoverlapping signals of the aromatic protons of Thi as 14.3 ± 0.8% for Oic[8], whereas for Pro[2] and Hyp[3] this can be estimated from the volumes of cross peaks as between 10 and 15%. ^{1}H NMR parameters of the main *all-trans* isomer together with assigned signals of the minor isomers are presented in Table 1. A random or extended conformation in water solution for compound B-9340 is in agreement with other observations for bradykinin and its agonists and antagonists (see refs 7, 14, and 44 and references therein).

A short dynamic run performed with the peptide immersed in water in the absence of any constraints also shows a large molecular flexibility. The resulting trajectory shows no trend for a preferred conformation or a preference for some backbone torsion angles. Averaging of the coordinates followed by minimization led to a structure with high values for most of the backbone torsion angles. The overall shape of such an averaged conformation of B-9340 in a water environment resembles an extended chain (Table 4, column W). This structure, of course, does not represent the only conformation or the most populated one in water.

In spectra measured in the SDS micellar environment, only one set of signals was seen. The ^{1}H NMR data are presented in Table 2, and the fingerprint part of the NOESY spectrum is given in Figure 5. The distance constraints are in Table 3. Several NOE cross peaks useful for structure elucidation and molecular modeling are present. There is a weak interaction between Hyp[3]αH and Thi[5]NH, another weak interaction between D-Igl[7]αH and Arg[9]NH, and a group of medium interactions between the heteroaromatic protons of Thi[5] and the benzylic and homobenzylic (β and γ) protons of D-Igl[7]. The first two interactions are of the type αH_i-NH_{i+2}, characteristic for β-turns. Both signals are weak, but they are reproducible at various temperatures and mixing times, and one of them, partly overlapping with another signal, can be clearly distinguished by selectively enhancing weighting, especially at low temperature (not shown). Additional useful information is the spatial proximity of the aromatic protons of Thi[5] to the β and γ protons of D-Igl[7]. Furthermore, the same intensities of NOE from Thi[5] to all four γ protons of D-Igl[7] are in agreement with free rotation and similar populations of conformations of the D-Igl[7] side chain as was concluded from the NOESY spectra measured in water. Because of the possibility of chemical exchange between pairs of γ protons of D-Igl, the conclusions about distances involving these atoms have to be treated carefully. The fact that the volumes of the cross peaks are independent of temperature in the range 15−35 °C and that calculated distances are comparable to those from Thi[5] to a single β proton of D-Igl led to the conclusion to use the γ protons of D-Igl for modeling. A decrease in intensity is observed in going from the 3′ to the 5′ protons of Thi[5] with the γ protons of D-Igl[7]; therefore molecular dynamic runs were started with the thiophene ring oriented with the sulfur away from D-Igl[7]. From some splittings of nonoverlapping signals of Oic[8] in water solution and from line shapes in the micellar environment, it is evident that the preferred conformation of the cyclohexane ring in both cases is a chair with axial protons $4_{pro\text{-}S}$, $5_{pro\text{-}R}$, $6_{pro\text{-}R}$, and $7_{pro\text{-}S}$ (broad quadruplets in water with $J \sim 13$ Hz or similarly shaped broad lines in the presence of micelles for axial

Table 4. Dihedral Angles (deg) and Energies (kcal/mol) of Selected Conformations from the Monte Carlo Search and from the Molecular Dynamic Runs of BK Antagonist B-9340

structure		M1[a]	M2[a]	W[b]	H[c]	C[d]	E[e]	N[f]
energy		143.4	144.0					
D-Arg	ψ	−115.1	−44.8	−137.7	−118.1	−108.8	−132.7	−127.6
	ω	178.6	−172.2	−178.7	172.6	176.6	166.3	169.4
Arg	ϕ	−70.3	−150.7	−157.0	−141.1	−149.5	−124.0	−136.1
	ψ	155.5	114.0	59.2	81.1	78.1	57.5	65.9
	ω	−167.8	−171.0	178.3	−178.7	175.8	−168.9	179.8
Pro	ϕ	−64.7	−70.9	−62.4	−52.4	−52.9	−31.4	−33.5
	ψ	112.3	−10.5	114.7	118.4	108.9	97.5	104.9
	ω	170.2	159.6	−174.0	177.0	179.1	171.2	167.7
Hyp	ϕ	−80.0	−90.9	−82.8	−74.9	−67.3	46.4	−61.2
	ψ	−178.5	−96.2	120.9	162.3	170.9	134.5	131.7
	ω	−167.1	171.6	−175.9	−161.9	−174.2	−160.9	−156.0
Gly	ϕ	118.4	77.4	−118.3	67.8	70.2	122.4	137.4
	ψ	−57.2	−60.5	78.7	48.1	29.8	−53.0	−43.4
	ω	166.4	−171.6	−176.3	168.9	176.0	164.0	154.2
Thi	ϕ	−172.4	−145.1	−123.3	119.9	127.3	178.1	175.6
	ψ	73.6	−99.1	110.0	86.9	93.5	138.4	114.5
	ω	160.9	−165.0	174.7	−171.4	158.5	157.6	164.8
Ser	ϕ	−77.5	−170.4	−100.7	−155.4	−127.4	−114.7	−102.2
	ψ	46.8	−28.2	127.4	39.0	43.7	48.0	43.5
	ω	−150.7	11.0	−179.2	−112.8	−129.8	−135.0	−155.0
D-Igl	ϕ	57.25	81.9	−112.1	20.5	53.5	60.5	75.3
	ψ	−161.1	5.1	55.2	−156.3	−176.6	−172.8	−152.4
	ω	−162.9	−150.9	179.0	−156.6	−166.8	−167.5	179.9
Oic	ϕ	−90.5	−93.5	−60.8	−97.4	−91.8	−82.2	−96.7
	ψ	49.0	71.0	117.0	48.4	44.1	36.5	62.6
	ω	−179.5	167.2	−166.3	176.5	−177.6	165.1	−169.7
Arg	ϕ	−153.9	−101.7	−135.8	−156.6	−140.8	−139.1	−158.4

[a] M1−M2, two lowest energy conformers from the Monte Carlo search in vacuum. [b] W, averaged and minimized structure from the MD run in water. [c] H, structure in micellar environment after heating and equilibration with constraints. [d] C, averaged and minimized structure in micellar environment with constraints. [e] E, end of unconstrained MD run in micellar environment. [f] N, averaged and minimized structure from the unconstrained MD run.

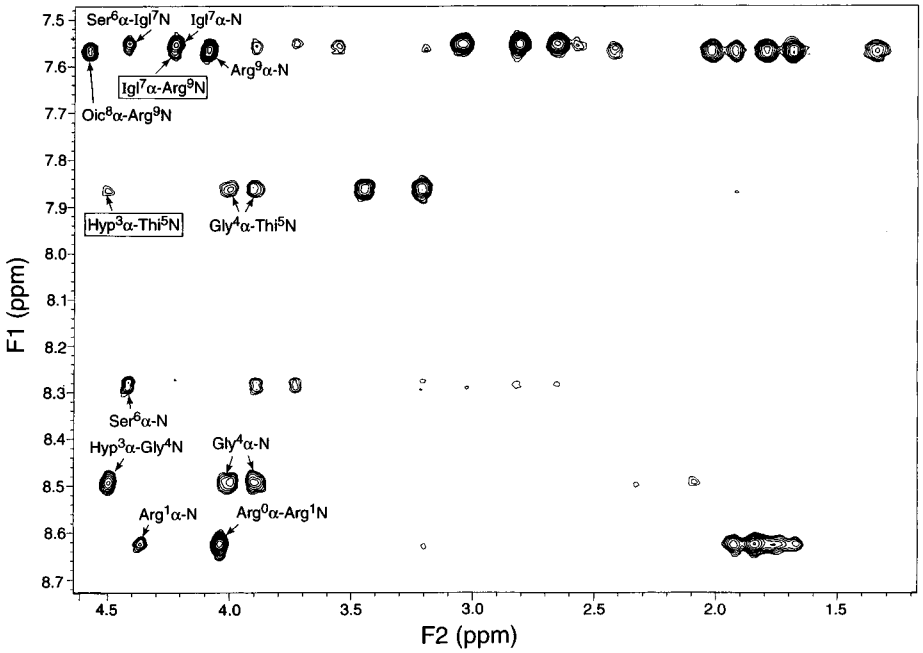

Figure 5. A part of the NOESY spectrum of BK antagonist B-9340 (7 mM) in 280 mM solution of SDS at 25 °C with a mixing time of 150 ms.

protons). This conformation of Oic[8], which is in agreement with the results after the dynamic run of HOE 140[14] was used as the starting point for molecular modeling.

According to Chou−Fasman rules[45,46] and other tools for prediction of secondary structure from sequence,[47,48] there is some probability of nonspecific turns at the N-terminus of the BK antagonist B-9340, specifically a very strong probability of a type II β-turn comprising residues 2−5 caused by proline and hydroxyproline residues, and a strong probability of a βII′-turn between residues 6−9 caused by the D-amino acid in position 7.

NH temperature coefficients provide information about the hydrogen bonding of these protons, usually with backbone or side-chain carbonyl groups. They are strongly dependent on experimental conditions (solvent, pH), but temperature coefficients close to and above −3 ppb/K are generally indicative of hydrogen bonding. In our case, the existence of two NH protons with low temperature dependence (Thi[5] and Arg[9], Table 2) is in

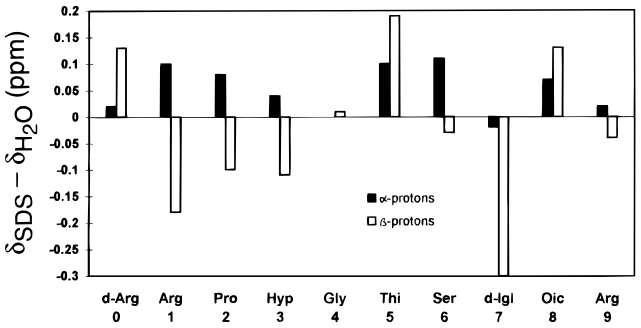

Figure 6. Difference between the chemical shifts of the α and β protons measured in SDS micellar solution and in water ($\delta_{SDS} - \delta_{water}$) in ppm.

agreement with β-turns comprising residues 2−5 and 6−9. On the other hand, the phenomenon of temperature dependence is based on exchange with exchangeable protons of solvent, so in the micellar environment, where some of the NH protons can be hardly accessible to the solvent, this may lead to incorrect conclusions about the structure. It is well-known that in nonpolar solvents such as $CDCl_3$ the temperature dependence of the backbone NH chemical shifts is very small, ranging from −1 to −3 ppb/K.[49] Chemical shifts of NH protons in B-9340 are highly temperature dependent, especially those near the N-terminus of the molecule. These results lead to the conclusion that most of the backbone is not very deeply buried in the micelle.

Similarly, proposals of backbone conformation can be based on proton chemical shifts. It is well-known that chemical shifts reflect secondary structure of peptides and proteins.[50] In the case of ^{1}H NMR shifts, this effect was elucidated from spectra of proteins with known structure[50] as well as calculated from the shielding of neighboring groups.[51] Differences between chemical shifts of α and β protons measured in a micellar environment and in water (taken as reference for random coil) are summarized in Figure 6. The differences in chemical shifts for the most affected central residues in turns support the prediction of β-turns in positions 2−5 and 6−9. There is also the possibility of other type II β-turns near the N-terminus of the decapeptide. As in the case of NH temperature dependence, these results must be treated with caution since part of the molecule can be in an aqueous environment whereas another part can be surrounded by nonpolar chains of SDS molecules.

The low intensities of $\alpha H_i - NH_{i+2}$ cross peaks lead to two possibilities: First of all, the molecule adopts more than one conformation and there is a low population of β-turns, or second, one conformer with a nonclassic or a distorted turn is present. All molecular modeling was carried out by supposing that the backbone of the molecule adopts one conformation. This is supported by the observation of all possible $NH_i - NH_{i+1}$ interactions in the NOESY spectra and by observation of only one isomer of the three proline-like residues (Pro[2], Hyp[3], and Oic[8]).

Recently, methods simulating a micellar environment and a membrane−water interface were developed (see refs 14, 52, and 53 and references therein). The methods used are time-consuming and require powerful computers. The use of biphasic cells[14] consisting of layers of water and CCl_4 and molecular dynamics allowed the conformation of the BK antagonist HOE-140 to be evaluated. The use of this biphasic mimetic also allowed the calculation of the orientation and the dynamics at the phase interface. This was extended to calculations of the unfolding of the peptide in H_2O. Finally, the refined structure was embedded in the apolar phase and the reorientation was studied in the biphasic system. The authors[14] employed computing facilities that included a Cray YMP computer, which is much more powerful than our Sun 4/470 system. We tried to find a simple solution for our hardware, software, and restricted computer time. As a reasonable compromise of many factors, a layer of 7 × 7 parallel-oriented molecules of octyl sulfate anions and the peptide solvated with a trimolecular shell of water was used. No constraints for water or detergent molecules were used to avoid destruction of the system. Such constraints greatly expand the computer time, and preliminary short dynamic runs performed at 500 K showed that some destruction of the system takes place but affects only those molecules of detergent lying in or near the corners of the initial matrix. The water shell and molecules of octyl sulfate lying near the peptide form a compact cluster. During the whole set of dynamic runs only three molecules of water and four molecules of octyl sulfate left the system.

We assumed that most of the folding in the molecule is caused by interactions of polar or charged groups in the non polar environment and that the micelle is able to change its shape according to the requirements of the peptide.[54] We then started our structure refinement with *in vacuo* simulation. The Monte Carlo search for the lowest energy conformers described above led to interesting results. Sixteen of the 20 best conformers exhibit broad folding in the molecule leading to orientation of all three arginine side chains and hydroxyl groups in Hyp[3] and Ser[6] to one side of the molecule. The best conformers were manually checked for short interatomic distances (about 2−3 Å) not found in NOESY spectra, and such structures were eliminated, for example the structure with a *cis* peptide bond between D-Igl[7] and Oic[8], with a short interatomic distance between α protons of both residues with no corresponding cross peak in the NOESY spectrum. Backbone torsion angles of the two best conformers are given in Table 4 in columns M1 and M2 together with their energies.

Two lowest energy conformers from the Monte Carlo search (column M1 in Table 4) were separately equilibrated giving structures with the biggest difference in backbone dihedral angles of 11°. The structure arising from conformer M1 was used for dynamic runs. The view of the starting system is presented in Figure 7A. During the heating, cooling, and equilibration periods it is possible to see the slow moving of the peptide toward the interface between phases. At the same time, some molecules of the detergent move from the wall of detergent into the water phase, thus approaching the positively charged guanidine moieties of the arginine residues. Hydrocarbon chains of detergent molecules simultaneously surround the hydrophobic parts of residues on both ends of the peptide (Pro[2], Hyp[3], Thi[5], D-Igl[7], Oic[8], and the chains of all three arginines). The position and orientation of the peptide molecule with respect to the interface was stabilized during a 30 ps equilibration period (adiabatic MD run at 300 K) as well as the overall

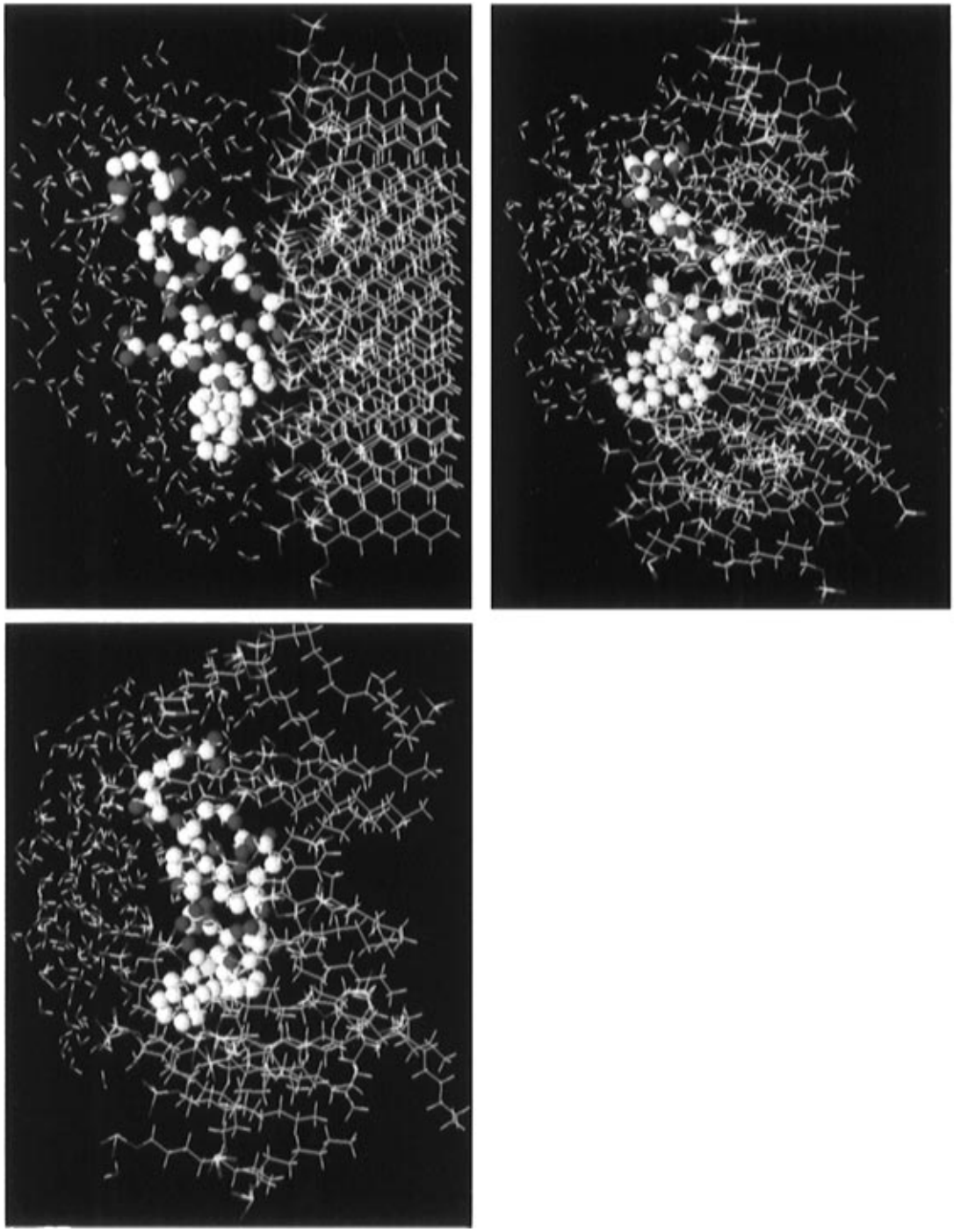

Figure 7. Views of the system used for the molecular simulation of BK antagonist B-9340. Backbone dihedral angles of the peptide in these three views are summarized in Table 4, columns M2, H, and N, respectively. (Top left, A) System before starting MD run. (Top right, B) System after equilibration period. (Bottom, C) Averaged and minimized system after unconstrained MD run (some detergent molecules not touching the peptide are deleted).

shape of the interface between the water phase and detergent molecules. No principal changes in positions of detergent molecules surrounding B-9340 were found in the trajectories following the equilibration period. The view of the system after equilibration is shown in Figure 7B and backbone dihedral angles are presented in Table 4, column H. At the end of equilibration, both β-turns are not fully developed, and most of the hydrogen bonds and charge−charge interactions are between polar groups of peptide and the water molecules or the negatively charged sulfate groups of detergent.

A molecular dynamic run of 80 ps with the application of all constraints listed in Table 3 caused the formation of two β-turns. Both turns were formed within the first 20 ps of the run. From the NOESY spectra it is not clear what types of turns are present. Residues without backbone NH hydrogens in positions 2, 3, and 8 do not provide information about NH−NH distances important for the determination of the turn type. Turns in B-9340 during molecular modeling initially were formed as type β II comprising residues Pro^2-Thi^5 and as type β II′ in residues Ser^6 to Arg^9. During all subsequent simulations these β-turns did not change. In some parts of the trajectory the turns are nearly ideal, stabilized by intramolecular hydrogen bonds; in other parts they are nonideal with disruption of the above-mentioned hy-

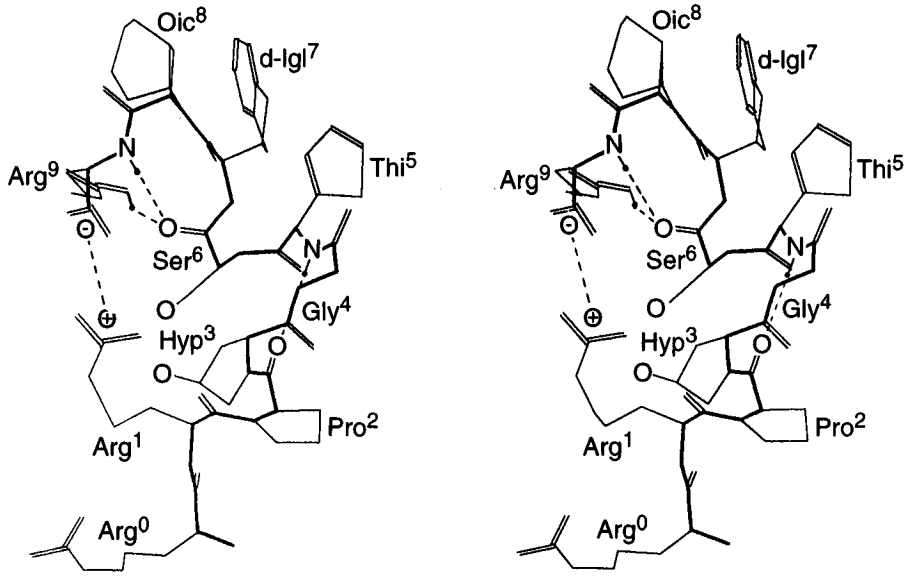

Figure 8. Stereoview of the conformation of BK antagonist B-9340 obtained from the molecular dynamic run. Hydrogen bonds and charge−charge interactions are indicated by dashed lines; backbone is indicated by bold lines. Backbone dihedral angles of the presented conformer are given in Table 4, column N.

drogen bonds. These structures are stabilized by hydrogen bonds to the water molecules and also to the guanidine group of Arg[9] in the case of the Ser[6] carbonyl. In the second half of the trajectory the salt bridge between the carboxyl of Arg[9] and guanidine moiety of Arg[1] was formed. This interaction persisted unchanged during nearly all subsequent simulations.

In Table 4, column C, are presented the backbone parameters for the averaged (whole constrained trajectory, 80 ps, 800 conformers) and minimized structure of B-9340. This structure differs only slightly from the structure obtained from the last 40 ps. Both turns are nonideal in the average conformation. The resulting structure suffers from big distortions of ω torsion angles in the middle part of the molecule. These distortions are probably caused by errors in some interproton NH−NH distance calculations for protons exchangeable with solvent and possible spin diffusion in the case of the unusual $NH_i-\alpha H_{i+1}$ distance constraint. This constraint was calculated from the small cross peak Ser[6]-NH-D-Igl[7] αH which occurs together with the huge cross peaks Ser[6]NH-D-Igl[7]NH and D-Igl[7]NH-D-Igl[7] αH. Only little improvement was achieved by minimization of the system without constraints.

Therefore, an unconstrained MD run of the system was performed for another 120 ps. Backbone torsion angles of the final conformation are presented in Table 4, column E. Great improvements in the distortions in the middle part of the molecule were found in nearly all conformers and also in the minimized and averaged structure obtained from the second half of the trajectory. The competition between intramolecular and intermolecular hydrogen bonding in β-turns described for the constrained run (see above) is unchanged; averaging and minimizing the second half of the trajectory led to the structure with a fully developed hydrogen bond in a type II β-turn involving residues 2−5. The hydrogen bond in a type II′ β-turn has competition in bonding of the Ser[6] carbonyl to the guanidine moiety of Arg[9]. A view of the averaged and minimized system is presented in Figure 7C. A schematic stereoview with intramolecular hydrogen bonds and a salt bridge is shown in Figure 8, and backbone dihedral angles are summarized in Table 4, column N. Details of this structure are in Brookhaven PDB file 1BDK.

Our results are different from those published recently for a similar bradykinin antagonist HOE 140, which differs from B-9340 only in the presence of the D-amino acid Tic (1,2,3,4-tetrahydroisoquinoline-3-carboxylic acid) in position 7; it was studied under nearly the same experimental conditions.[14] NOESY measurements resulted in one interesting distance constraint (Gly[4]NH−Oic[8]αH). Modeling including that constraint led to a structure with two β-bends comprising residues 2−5 and 6−9 as well as a folding in the middle part of the molecule. The authors showed no direct experimental proof for β-turns. That folding, which is in agreement with our experimental data, arises from molecular modeling. We have found no cross peak between Gly[4]NH and Oic[8]αH even when we endeavored to find it in the noise after using various signal to noise ratio-enhancing weighting functions. In our case we have clearly resolved α-protons of Hyp[3] and Oic[8] (4.51 and 4.59 ppm, respectively). In the case of HOE 140 it is possible to have overlap between Gly[4]NH−Hyp[3]αH and Gly[4]NH−Oic[8]αH (4.50 and 4.49 ppm). It is possible to reconstruct the modeled backbone from the published data, and after optimizing the positions of backbone hydrogens by short minimization in vacuo (500 steps, conjugate gradient, rigid positions of backbone carbon and nitrogen atoms, all $\chi_1 = +60°$), it was seen that the distance between Gly[4]NH and Oic[8]αH is about 2.77 Å and the distance between Gly[4]NH and Hyp[3]αH is about 2.08 Å. As well, such a highly folded structure should have other medium and long-range interactions leading to NOE cross peaks between Hyp[3]αH and Thi[5]NH (2.81 Å) or Gly[4]NH and Arg[9]NH (3.01 Å).

Of course, these are two different compounds, but the chemical shifts of most of the protons are nearly the same for HOE 140 and B-9340. Big differences are observed only in the case of the nonequivalent D-amino acids in position 7 (Tic versus D-Igl), in Ser[6] and in the aromatic protons of Thi[5]. The protons bonded to the thiophene ring are in our case near the aromatic ring

of D-Igl[7], as shown from the NOESY spectra (see above). The aromatic ring of D-Igl can rotate freely, whereas the orientation of the Tic aromatic ring in HOE 140 is determined by the backbone conformation. All other protons are shifted only very slightly; for example the differences in backbone hydrogens (NH and CαH) are maximum value 0.11 ppm, average deviation for 13 protons is 0.04 ppm; difference in other hydrogens are maximum value 0.23 ppm, average deviation for 39 protons is 0.06 ppm. Such small changes in chemical shifts lead to the assumption that both compounds adopt a similar conformation in a micellar environment and also a similar position and orientation with respect to the interface between nonpolar and aqueous phases. The structure published for HOE-140 and our structure for B-9340 have many similarities. Both bradykinin antagonists adopt the same β-turns and the side chain of Arg^0 is apart of the rest of the molecule and is not involved in structural elements. On the other hand, differences are observed in the broad folding of the middle part of the decapeptide and in the stabilization of the structural elements by hydrogen bonds.

Conclusions

According to proton 2D-NMR measurements and molecular modeling, the bradykinin antagonist B-9340 has no stable secondary structure in water solution and contains about 10−15% *cis* peptide bonds arising from proline-like residues Pro, Hyp, and Oic. On the other hand, in the presence of SDS micelles, NMR reveals the existence of two β-turns and further provides a relatively small number of connectivities that were useful for molecular modeling. We performed molecular dynamic runs of the peptide in an environment consisting of a layer of octyl sulfate anions and water. According to our molecular modeling, the structure of the bradykinin antagonist B-9340 in the micellar environment is characterized by a nonideal βII-turn comprising residues Pro^2-Thi^5, a nonideal βII′-turn comprising residues Ser^6-Arg^9, and broad folding in the middle part of the molecule. Observed β-turns are in agreement with the CD curves. The structure is stabilized by a group of intramolecular hydrogen bonds and by a salt bridge between the guanidine moiety of Arg^1 and the carboxyl group of Arg^9. The middle part of the peptide is buried in the micelle where a broad pocket filled with water is formed.

Acknowledgment. Financial support by the Natural Sciences and Engineering Research Council of Canada, the University of Alberta, and USNIH Grant HL26284 is gratefully acknowledged.

References

(1) Goodfriend, T. L.; Ball, D. L. Radioimmunoassay of bradykinin: Chemical modification to enable use of radioactive iodine. *J. Lab. Clin. Med.* **1969**, *73*, 501−511.
(2) Regoli, D.; Barabe, J. Pharmacology of bradykinin and related kinins. *Pharmacol. Rev.* **1980**, *32*, 1−46.
(3) Farmer, S. G.; Burch, R. M. The pharmacology of bradykinin receptors. In *Bradykinin Antagonists, Basic and Clinical Research*; Burch, R. M., Ed.; Marcel Dekker: New York, 1991; pp 1−31.
(4) Mason, D. T.; Melmon, K. L. Abnormal forearm vascular responses in the carcinoid syndrome: The role of kinins and kinin-generating system. *J. Clin. Invest.* **1966**, *45*, 1685−1699.
(5) Proud, D.; Reynolds, C. J.; Lacapra, S.; Kagey-Sobotka, A.; Lichtenstein, L. M.; Naclerio, R. M. Nasal provocation with bradykinin induces symptoms of rhinovirus and a sore throat. *Am. Rev. Respir. Dis.* **1988**, *137*, 613−616.
(6) Naclerio, R. M.; Proud, D.; Lichtenstein, L. M.; Kagey-Sobotka, A.; Hendley, J. O.; Sorrentino, J.; Gwaltney, J. M. Kinins are generated during experimental rhinovirus colds. *J. Infect. Dis.* **1988**, *157*, 133−142.
(7) Lee, S. C.; Russell, A. F.; Laidig, W. D. Three dimensional structure of bradykinin in SDS micelles. *Int. J. Pept. Protein Res.* **1990**, *35*, 367−377.
(8) Kyle, D. J.; Martin, J. A.; Farmer, S. G.; Burch, R. M. Design and conformational analysis of several highly potent bradykinin receptor antagonists. *J. Med. Chem.* **1991**, *34*, 1230-1233.
(9) Kyle, D. J.; Hicks, R. P.; Blake, P. R.; Klimkowski, V. J. Conformational properties of bradykinin and bradykinin antagonists. In *Bradykinin Antagonists, Basic and Clinical Research*; Burch, R. M., Ed.; Marcel Dekker: New York, 1991, pp 131−146.
(10) Cann, J. R.; Liu, X.; Stewart, J. M.; Gera, L.; Kotovych, G. A CD and an NMR study of multiple bradykinin conformations in aqueous trifluoroethanol solutions. *Biopolymers* **1994**, *34*, 869−878.
(11) Burch, R. M.; Farmer, S. G.; Steranka, L. R. Bradykinin receptor antagonists. *Med. Res. Rev.* **1990**, *10*, 237−269.
(12) Kyle, D. J.; Blake, P. R.; Smithwick, D.; Green, L. M.; Martin, J. A.; Sinsko, J. A.; Summers, M. F. NMR and computational evidence that high-affinity bradykinin receptor antagonists adopt C-terminal β-turns. *J. Med. Chem.* **1993**, *36*, 1450−1460.
(13) Liu, X.; Stewart, J. M.; Gera, L.; Kotovych, G. Proton magnetic resonance studies of bradykinin antagonists. *Biopolymers* **1993**, *33*, 1237−1244.
(14) Guba, W.; Haessner, R.; Breipohl, G.; Henke, S.; Knolle, J.; Santagada, V.; Kessler, H. Combined approach of NMR and molecular dynamics within a biphasic membrane mimetic: Conformation and orientation of the bradykinin antagonist HOE 140. *J. Am. Chem. Soc.* **1994**, *116*, 7532−7540.
(15) Schwyzer, R. Estimated conformation, orientation, and accumulation of dynorphin A-(1-13)-tridecapeptide on the surface of neutral lipid membranes. *Biochemistry* **1986**, *25*, 4281−4286.
(16) Shelley, J.; Watanabe, K.; Klein, M. L. Simulation of a sodium dodecylsulfate micelle in aqueous solution. *Int. J. Quantum Chem.: Quantum Biol. Symp.* **1990**, *17*, 103−117.
(17) Stewart, J. M.; Young, J. D. *Solid Phase Peptide Synthesis*; Pierce Chemical Co.: Rockford, IL, 1984.
(18) Stewart, J. M.; Vavrek, R. J. Chemistry of peptide B2 bradykinin antagonists. In *Bradykinin Antagonists, Basic and Clinical Research*; Burch, R. M., Ed.; Marcel Dekker: New York, 1991; pp 51−96.
(19) Fournier, A.; Wang, C.-T.; Felix, A. M. Applications of BOP reagent in solid phase synthesis. *Int. J. Pept. Protein Res.* **1988**, *31*, 86−97.
(20) Porter, T. H.; Shive, W. **dl**-2-indaneglycine and **dl**-β-trimethylsilylalanine. *J. Med. Chem.* **1968**, *11*, 402−403.
(21) States, D. J.; Haberkorn, R. A.; Ruben, D. J. A two-dimensional nuclear Overhauser experiment with pure absorption phase in four quadrants. *J. Magn. Reson.* **1982**, *48*, 286−292.
(22) Braunschweiler, L.; Ernst, R. R. Coherence transfer by isotropic mixing: Application to proton correlation spectroscopy. *J. Magn. Reson.* **1983**, *53*, 521−528.
(23) Bax, A.; Davis, D. G. MLEV-17-based two-dimensional homonuclear magnetization transfer spectroscopy. *J. Magn. Reson.* **1985**, *63*, 355−360.
(24) Bothner-By, A. A.; Stephens, R. L.; Lee, J.; Warren, C. D.; Jeanloz, R. W. Structure determination of a tetrasaccharide: Transient nuclear Overhauser effects in the rotating frame. *J. Am. Chem. Soc.* **1984**, *106*, 811−813.
(25) Bax, A.; Davis, D. G. Practical aspects of two-dimensional transverse NOE spectroscopy. *J. Magn. Reson.* **1985**, *63*, 207−213.
(26) Aue, W. P.; Bartholdi, E.; Ernst, R. R. Two-dimensional spectroscopy. Application to nuclear magnetic resonance. *J. Chem. Phys.* **1976**, *64*, 2229−2246.
(27) Neuhaus, D.; Williamson, M. P. *The nuclear Overhauser effect in structural and conformational analysis*; VCH Publishers, Inc.: New York, 1989.
(28) Wüthrich, K. *NMR of Proteins and Nucleic Acids*; Wiley-Interscience: New York, 1986.
(29) Bax, A.; Subramanian, S. Sensitivity-enhanced two-dimensional heteronuclear shift correlation NMR spectroscopy. *J. Magn. Reson.* **1986**, *67*, 565−569.
(30) Wüthrich, K.; Billeter, M.; Braun, W. Pseudo-structures for the 20 common amino acids for use in studies of protein conformations by measurements of intramolecular proton-proton distance constraints with nuclear magnetic resonance. *J. Mol. Biol.* **1983**, *169*, 949−961.
(31) Gasteiger, J.; Marsili, M. Iterative partial equalization of orbital electronegativity - a rapid access to atomic charges. *Tetrahedron* **1980**, *36*, 3219−3228.
(32) Cann, J. R.; Vatter, A.; Vavrek, R. J.; Stewart, J. M. Interaction of bradykinin with sodium dodecyl sulfate and certain acidic lipids. *Peptides* **1986**, *7*, 1121−1130.

(33) Appu Rao, A. G.; Stewart, J. M.; Vavrek, R. J.; Sillerud, L. O.; Fink, N. H.; Cann, J. R. A fluorometric study of the interaction of bradykinin with lipids. *Biochim. Biophys. Acta* **1989**, *997*, 278−283.
(34) Chen, G. C.; Yang, J. T. Two-point calibration of circular dichrometer with d-10-camphorsulfonic acid. *Anal. Lett.* **1977**, *10*, 1195−1207.
(35) Woody, R. W. Studies of theoretical circular dichroism of polypeptides: Contributions of β-turns. In *Peptides, Polypeptides and Proteins*; Blout, E. R., Bovey, F. A., Goodman, M., Loton, N., Eds.; John Wiley: New York, 1974; pp 338−350.
(36) Kawai, M.; Fasman, G. A model β turn. Circular dichroism and infrared spectra of a tetrapeptide. *J. Am. Chem. Soc.* **1978**, *100*, 3630−3632.
(37) Gierasch, L. M.; Deber, C. M.; Madison, V.; Niu, C.-H.; Blout, E. R. Conformation of (X-**L**-Pro-Y)$_2$ cyclic hexapeptides. Preferred β-turn conformers and implications for β turns in proteins. *Biochemistry* **1981**, *20*, 4730−4738.
(38) Marlborough, D. I.; Ryan, J. W.; Felix, A. M. Conformation of bradykinin in relation to solvent environment. *Adv. Exp. Med. Biol.* **1976**, *70*, 43−51.
(39) Schwyzer, R. 100 Years lock-and-key concept: Are peptide keys shaped and guided to their receptors by the target cell membrane? *Biopolymers (Pept. Sci.)* **1995**, *37*, 5−16.
(40) Tanford, C.; Reynolds, J. A. Structure and assemply of human serum lipoproteins. In *Chemistry and Physiology of Human Plasma Proteins*; Bing, D. H., Ed.; Pergamon Press: New York, 1979; pp 111−126.
(41) Henry, G. D.; Sykes, B. D. *Methods to Study Membrane Protein Structure in Solution Methods in Enzymology*; James, T. L., Oppenheimer, N. J., Eds.; Academic Press: New York, 1994; Vol. 239, pp 515−535.
(42) Bösch, C.; Brown, L. R.; Wüthrich, K. *Biochim. Biophys. Acta* **1980**, *603*, 298−312.
(43) Reiss-Husson, F.; Luzzati, V. *J. Phys. Chem.* **1964**, *68*, 3504−3511.
(44) Denys, L.; Bothner-by, A. A.; Fisher, G. H.; Ryan, J. W. Conformational diversity of bradykinin in aqueous solution. *Biochemistry* **1982**, *21*, 6531−6536.
(45) Chou, P. Y.; Fasman, G. D. Prediction of β-turns. *Biophys. J.* **1979**, *26*, 367−384.
(46) Wilmot, C. M.; Thornton, J. M. Analysis and prediction of the different types of β-turn in proteins. *J. Mol. Biol.* **1988**, *203*, 221−232.
(47) Kessler, H.; Bats, J. W.; Griesinger, C.; Koll, S.; Will, M.; Wagner, K. Peptide conformations. 46. Conformational analysis of a superpotent cytoprotective cyclic somatostatin analogue. *J. Am. Chem. Soc.* **1988**, *110*, 1033−1049.
(48) Rose, G. D.; Gierasch, L. M.; Smith, J. A. Turns in peptides and proteins. *Adv. Protein Chem.* **1985**, *37*, 1−109.
(49) Stevens, E. S.; Sugawara, N.; Bonora, G. M.; Toniolo, C. Conformational analysis of linear peptides. Temperature dependence of NH chemical shifts in chloroform. *J. Am. Chem. Soc.* **1980**, *102*, 7048−7050.
(50) Wishart, D. S.; Sykes, B. D.; Richards, F. M. Relationship between nuclear magnetic resonance chemical shift and protein secondary structure. *J. Mol. Biol.* **1991**, *222*, 311−333.
(51) Ösapay, K.; Case, D. A. Analysis of proton chemical shifts in regular secondary structure of proteins. *J. Biomol. NMR* **1994**, *4*, 215−230.
(52) Bassolino-Klimas, D.; Alper, H. E.; Stouch, T. R. Solute diffusion in lipid bilayer membranes: An atomic level study by molecular dynamics simulation. *Biochemistry* **1993**, *32*, 12624−12637.
(53) Heller, H.; Schaefer, M.; Schulten, K. Molecular dynamics simulation of a bilayer of 200 lipids in the gel and in the liquid-crystal phases. *J. Phys. Chem.* **1993**, *97*, 8343−8360.
(54) Papavoine, C. H. M.; Konings, R. N. H.; Hilbers, C. W.; van de Ven, F. J. M. Location of M13 coat protein in sodium dodecyl sulfate micelles as determined by NMR. *Biochemistry* **1994**, *33*, 12990−12997.

JM950485F